International Journal of Industrial Ergonomics 53 (2016) 37–47

Contents lists available at ScienceDirect

International Journal of Industrial Ergonomics

journal homepage: www.elsevier.com/locate/ergon

Simulation of lifting motions using a novel multi-objective optimization approach

Jiahong Song [a], Xingda Qu [b, *], Chun-Hsien Chen [a]

[a] School of Mechanical and Aerospace Engineering, Nanyang Technological University, Singapore
[b] Institute of Human Factors and Ergonomics, College of Mechatronics and Control Engineering, Shenzhen University, Shenzhen, China

ARTICLE INFO

Article history:
Received 2 February 2015
Received in revised form
12 May 2015
Accepted 12 October 2015
Available online xxx

Keywords:
Lifting
Human motion simulation
Multi-objective optimization
Physical effort
Load motion smoothness
Age

ABSTRACT

In this study, a novel lifting motion simulation model was developed based on a multi-objective optimization (MOO) approach. Two performance criteria, minimum physical effort and maximum load motion smoothness, were selected to define the multi-objective function in the optimization procedure using a weighted-sum MOO approach. Symmetric lifting motions performed by younger and older adults under varied task conditions were simulated. The results showed that the proposed MOO approach led to up to 18.9% reductions in the prediction errors compared to the single-objective optimization approach. This finding suggests that both minimum physical effort and maximum load motion smoothness play an important role in lifting motion planning. Age-related differences in the mechanisms for planning lifting motions were also investigated. In particular, younger workers tend to rely more on the criterion of minimizing physical effort during lifting motion planning, while maximizing load motion smoothness seems to be the dominant objective for older workers.

Relevance to industry: Lifting tasks are closely associated with occupational low back pain (LBP). In this study, a novel lifting motion simulation model was developed to facilitate the analysis of lifting biomechanics and LBP prevention. Age-related differences in lifting motion planning were discussed for better understanding LBP injury mechanisms during lifting.

1. Introduction

Low back pain (LBP) is one of the most prevalent and costly occupational injuries. In the US, the lifetime prevalence of LBP is over 60% (Krismer and van Tulder, 2007), and the corresponding annual costs exceed $100 billion (Katz, 2006). Manual lifting is a major risk factor for occupational LBP (Garg and Moore, 1992; Hoy et al., 2010), mainly because of the high loads imposed on the lumbar spine during lifting. Therefore, to well address the occupational LBP problem, there is a need for biomechanical analysis on the lifting task, including examining whole-body motions/postures, and estimating the loads imposed onto the body musculoskeletal system (Chaffin et al., 2006).

Many biomechanical models have been developed to estimate the loads exerted onto the human body (e.g., the low back joint moments and forces) during lifting tasks (Chaffin et al., 2006). Whole-body motions always become a necessary input to these models. The traditional way to collect actual human motions is using photographic, optical or inertial measurement systems in the field or lab-based experiment, which is time-consuming and usually results in high financial cost. The use of dynamic motion simulation models has recently evolved into a useful technology which can help predict human motions and reduce the time and costs spent on actual motion data collections (Abdel-Malek et al., 2006; Chaffin, 2005).

A majority of motion simulation models are based on the optimization principle. Various types of human motions, such as reaching (Jung et al., 1995; Jung and Shin, 2010; Mi et al., 2009), lifting (Lin et al., 1999) and walking (Xiang et al., 2009), have been predicted by these models. In these models, the central nervous system (CNS) is assumed to plan human motions using certain performance criteria. These criteria are then used to define objective functions in the optimization procedure to predict human motions. Many performance criteria have been proposed for lifting motion simulation, such as minimum efforts (Gündogdu et al.,

* Corresponding author. Institute of Human Factors and Ergonomics, College of Mechatronics and Control Engineering, Shenzhen University, 3688 Nanhai Avenue, Shenzhen, Guangdong Province 518060, China.
E-mail address: quxd@szu.edu.cn (X. Qu).

http://dx.doi.org/10.1016/j.ergon.2015.10.002
0169-8141/

2005; Hsiang and Ayoub, 1994; Lin et al., 1999), maximum dynamic stability (Abedi et al., 2012; Dysart and Woldstad, 1996), minimum low back spinal forces (Xiang et al., 2012a), and maximum load motion smoothness (Hsiang and McGorry, 1997).

One major limitation of the optimization-based models is the difficulty in identifying the 'true' performance criteria. This limitation can result in inaccurate and unrealistic predicted motions. To address this limitation, hybrid approaches which incorporate actual human motions into the optimization have been proposed in recent research (Pasciuto et al., 2014; Song et al., 2015; Xiang et al., 2012b). For instance, Pasciuto et al. (2014) and Xiang et al. (2012b) simulated human motions by minimizing the weighted-sum value of a knowledge-based and a data-based objective function. The knowledge-based objective function was defined based on the minimum energy criterion, and the data-based objective function was defined as the minimum difference between the actual and predicted motions. In our prior work (Song et al., 2015), a hybrid optimization-based model was proposed for lifting motion simulation, in which minimum physical effort was used as the performance criterion, and the simulated joint angular velocities were bounded by the time-functional constraints determined by actual motion data.

Chang et al. (2001) suggested that more than one performance criterion might be needed to better predict and explain the lifting behaviour. However, few studies in the existing literature applied more than one performance criterion in their motion simulation. To the best of our knowledge, the only study that used multiple performance criteria for lifting motion simulation was conducted by Xiang et al. (2010) who used a multiple objective optimization approach (MOO) to examine the relative effects of minimum dynamic effort and maximum stability for lifting motion planning. Xiang et al. (2010) found that the MOO approach did not lead to significant improvements on the simulation accuracy compared to the single-objective optimization approach which used the minimum dynamic effort as a single performance criterion. Thus, they suggested that the maximum stability may not be an effective performance criterion for lifting motion simulation, and there is a need to further investigate alternative performance criteria which can be used in the MOO approach for better lifting motion simulation.

Another limitation of the existing models for lifting motion simulation is that they were only used to predict motions for young and/or middle-aged (20–40 years) adults (Chang et al., 2001; Dysart and Woldstad, 1996; Hsiang and McGorry, 1997; Lin et al., 1999; Xiang et al., 2010). Lifting motions of older adults (>55 years) have not been extensively studied using the motion simulation method. In fact, previous experimental studies showed significant distinctions in lifting motion patterns between young and older adults (Song and Qu, 2014a, b), which implies that there exist age-related differences in the mechanisms for planning lifting motions.

To address the limitations of the existing lifting motion simulation models, the objectives of the present study are twofold. First, we aimed to propose a novel lifting motion simulation model using the MOO approach. The second objective was to investigate age-related differences in the mechanisms for lifting motion planning using the proposed lifting simulation model. Specifically, the hybrid model proposed in the prior work (Song et al., 2015) was further developed, in which two performance criteria, including minimum physical effort and maximum smoothness of the external load motion, were investigated. The objective function in the MOO was defined as the weighted sum of the performance measures derived from these two criteria. Lifting motions of younger and older adults were simulated separately to examine age effects on lifting motion planning mechanisms.

2. Actual lifting data collection

Actual lifting motion data from the prior work (Song and Qu, 2014a) were used for the model development and evaluation. Eleven younger participants (six males and five females) aged between 20 and 30 years old and twelve older participants (seven males and five females) aged over 55 years old were recruited from the university and local community. All of them were free from any musculoskeletal disorders in the last six months. The demographic information about their age, height, body weight and maximum lifting capacity (MLC) was listed in Table 1. All participants signed the consent form approved by the Nanyang Technological University Institutional Review Board before the data collection.

Before lifting motion data collection, participants conducted an isokinetic lifting test to measure their MLC using a commercial dynamometer (Biodex System 4 Pro, Shirley, NY, USA). After the MLC measurement, 31 reflective markers were placed on the selected body landmarks of each participant, and the whole-body lifting motions were measured using an eight-camera optoelectronic motion capture system (Motion Analysis Eagle System, Santa Rosa, CA, USA). The MLC measurement protocol and the marker placement can be found in Song and Qu (2014a).

During the lifting task, participants lifted a load from the floor to a shelf (Fig. 1). The lifted load was a square box (length × width × depth: 0.34 m × 0.24 m × 0.26 m) with two handles on its sides. Both the box and the shelf were placed directly in front of participants before lifting. The distance from the shelf edge to the participants' standing point (i.e. the middle point of the two ankle joints) was 58 cm. The initial horizontal distance from the box centre to participants' standing point was 40 cm. Three shelf heights (wrist, elbow and shoulder during the erect stance) and three load weights (5%, 15% and 25% of participants' MLC) were involved in the experiments. Therefore, there were nine lifting task conditions (3 shelf heights × 3 load weights) for each participant. These task conditions were randomly ordered during experiment, and three repetitions were performed for each task condition. Before each lifting trial, participants were informed of the lifted load weight and the destination height. Participants were not allowed to move their feet during lifting, and they were instructed to lift the box by holding its handles and using self-selected lifting strategies and speeds. Prior to data collection, participants were provided with a practice session to get familiar with the lifting protocol. To minimize fatigue effects, a 30-second break (standing without load) was given after every lifting trial.

The motion data from one older male participant and 41 lifting trials from other 11 participants were excluded because of the significant asymmetric movement patterns. The remaining data were divided into two sets for the purposes of model development and evaluation, respectively. Specifically, the lifting motions (totally 315 trials) from 12 participants were selected to formulate a database for model development. These 12 participants consist of 6 younger (age: 23.3(2.1), height: 168.2(8.5) cm, weight: 52.3(4.7) kg) and 6 older (age: 64.5(5.24), height: 163.7(7.7) cm, weight: 61.3(11.5) kg), and each age group contains 3 males and 3 females. The lifting motions (totally 238 trials) performed by the other 10 participants (5 younger and 5 older) were used for model evaluation. Both the younger (age: 24(1.9), height: 165.6(4.5) cm, weight: 57.4(8.2) kg) and older (age: 68.6(5.6), height: 159.6(6.9) cm, weight: 58(7.3) kg) age groups contain three males and two females.

3. The lifting motion simulation model using the MOO approach

Symmetric lifting (i.e., in the sagittal plane) is very common in

Table 1
Demographic information of participants.

	Young		Old	
	Male	Female	Male	Female
	Mean (SD)	Mean (SD)	Mean (SD)	Mean (SD)
Age (years)	25.0 (1.3)	22.0 (1.4)	68.1 (5.6)	63.2 (4.8)
Height (cm)	171.5 (5.3)	161.6 (4.3)	168.4 (8.7)	156.4 (3.4)
Body weight (kg)	57.3 (8.6)	51.4 (3.3)	65.1 (12.3)	55.6 (2.3)
Maximum lifting capacity (kg)	32.9 (7.3)	19.0 (5.0)	26.1 (13.9)	16.7 (5.7)

Fig. 1. A participant performing a lifting task in the experiment.

occupational settings, therefore this model focuses on simulating two-dimensional (2-D) lifting motions. The inputs of the model include the lifting task conditions (i.e., the lifted load weight, the initial and final load positions), the lifter's attributes (i.e., age, gender, body weight and segment lengths), the total lifting time duration and the starting and ending body postures. Specifically, similar with previous studies (Chang et al., 2001; Hsiang and Ayoub, 1994; Lin et al., 1999; Qu and Nussbaum, 2009), the lifting time duration and the starting and ending body postures are specified by the corresponding actual motion data. Besides, the values of the weighting parameters for the MOO approach are also specified before simulation. The output of the model is the simulated motions which are represented as the whole-body joint angular trajectories (angle–time functions). The whole model is composed of four components: a lifting motion database, a physical human body model, an optimization model, and a joint angular trajectory model. The model structure and the simulation process are illustrated in Fig. 2. The lifting motion database is constructed by the motion data for model development (Please see Section 2). The following presents the details of the other components and the simulation process.

3.1. Physical human body model

The human body during symmetric lifting is represented by a 2-D five-segment linkage model. Fig. 3(a) shows the segment configuration and the coordinate system of the linkage model. The segments of the model include the forearm, upper arm, trunk, thigh and shank ($L_1 \sim L_5$). The mass of the head and neck are integrated into the trunk segment, and these three body parts are combined as one rigid link. The inertia parameters of the segments (i.e., the mass, the moment of inertia and the centre of mass (COM) position of each segment) are determined according to de Leva (1996). The five joints from the elbow to ankle ($J_1 \sim J_5$) are modelled as revolute joints with one degree of freedom. The joint centre positions are determined by the sagittal projections of the corresponding reflective markers (Song and Qu, 2014a). Therefore, given the segment lengths, the body configuration at any time moment during lifting can be specified with the five joint angles (θ_i, $i = 1, \ldots, 5$) which are defined based on the orientation of the corresponding segments with respect to the horizontal axis X.

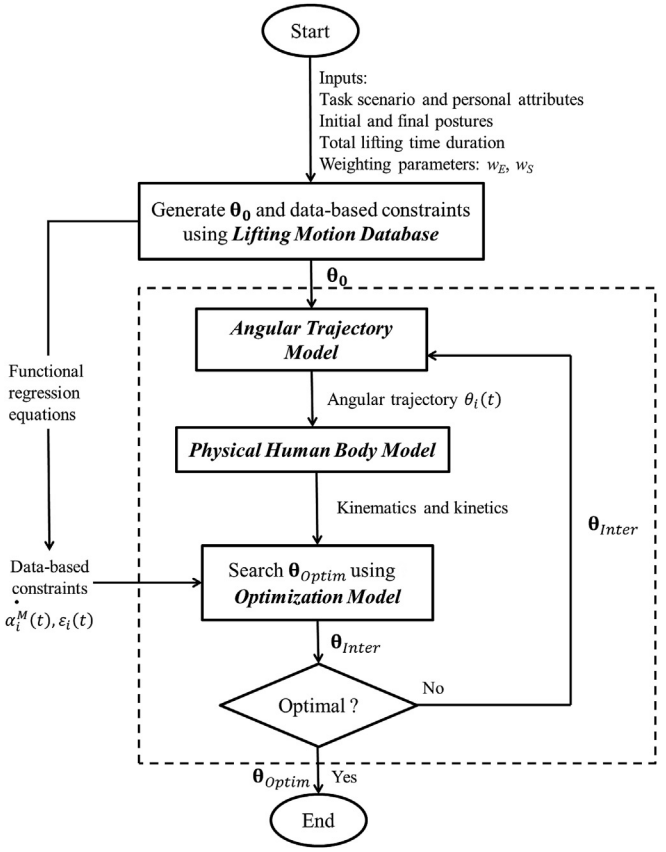

Fig. 2. The structure of the simulation model and the simulation process.

Given the lifted load weight, the whole-body kinematics, and the segments' lengths and inertia parameters, the joint reaction forces and moments can be calculated by analysing each body segment in a top–down sequence (i.e., forearm → upper

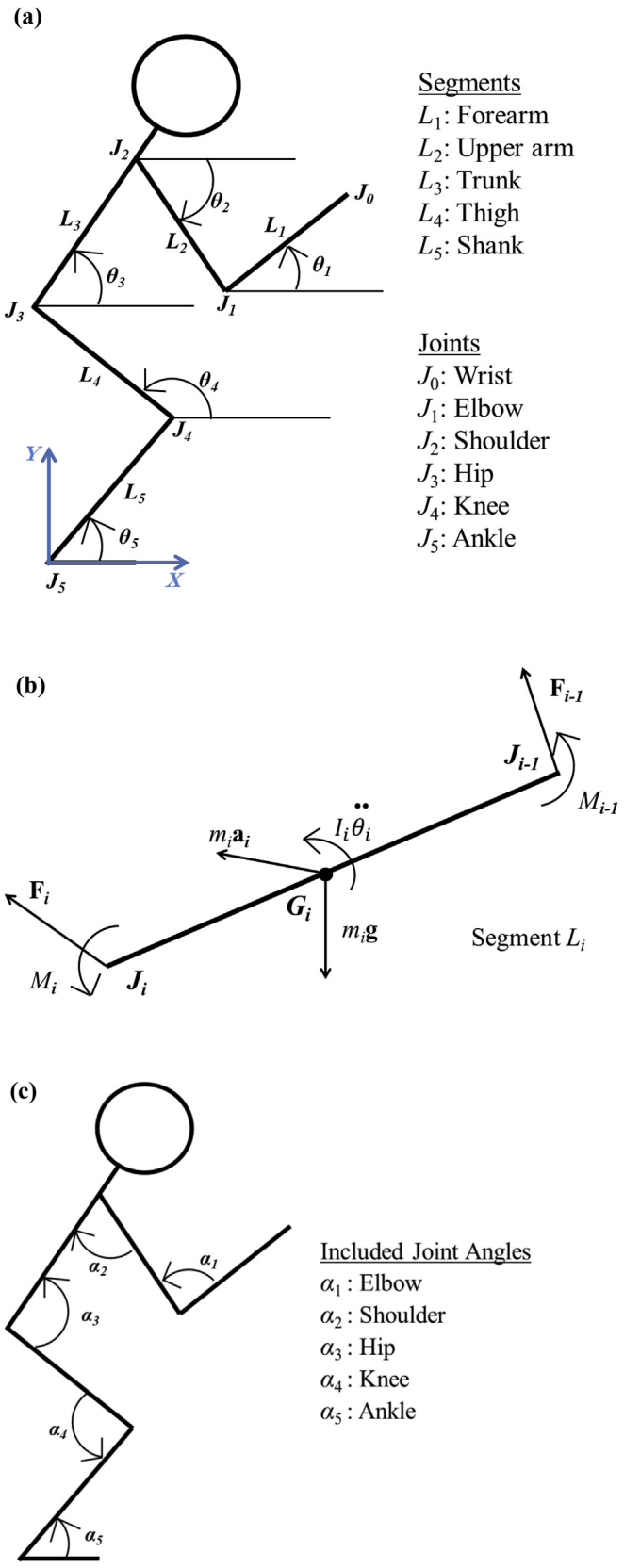

Fig. 3. The Human Body Linkage Model: (a) Human linkage model and coordinate system; (b) The free-body diagram of a segment with its joint reaction forces and moments; (c) The definition of the included joint angles.

arm → trunk → thigh → shank) using inverse dynamics. Fig. 3(b) shows a free-body diagram of one segment L_i, whose joint reaction forces and moments can be calculated by the following equations of motion (Eq. (1)):

$$\begin{aligned} &\mathbf{F}_i - \mathbf{F}_{i-1} + m_i\mathbf{g}_i = m_i\mathbf{a}_i \\ &M_i - M_{i-1} - \mathbf{r}_{Gi,Ji-1} \times \mathbf{F}_{i-1} + \mathbf{r}_{Gi,Ji} \times \mathbf{F}_i = I_i \ddot{\theta}_i \end{aligned} \tag{1}$$

where $\mathbf{F}_i$ and M_i are the force vector and moment acting at the *i-th* joint (J_i) onto the *i-th* segment (L_i), respectively; $\mathbf{r}_{Gi,Ji-1}$ and $\mathbf{r}_{Gi,Ji}$ are the vectors pointing from the COM (G_i) of the segment L_i to the joint J_{i-1} and J_i, respectively; $\mathbf{g}$ is the gravity vector; m_i and I_i are the mass and moment of inertia of the segment L_i, respectively; $\mathbf{a}_i$ is the linear acceleration of the COM G_i; $\ddot{\theta}_i$ is the angular acceleration of the segment L_i; and $\times$ denotes a vector product.

3.2. Optimization model

In this study, human motions are simulated by solving a nonlinear optimization problem. Lifting motions are assumed to be governed by two performance criteria (i.e., minimum physical effort and maximum smoothness of the lifted load motion). The minimum physical effort is associated with reduced energy expenditure during lifting (Fogleman and Smith, 1995), and has been extensively used for lifting motion simulation (Chang et al., 2001; Hsiang and Ayoub, 1994; Lin et al., 1999; Xiang et al., 2010). The maximum load motion smoothness has also been selected as a performance criterion for lifting motion simulation, as this criterion is associated with reduced low back load during symmetric lifting (Hsiang and McGorry, 1997) which is a critical issue in lifting motion control. Besides, Flash and Hogan (1985) indicated that achieving the smoothest motion may be one underlying objective of the CNS when planning human motions, because motions tended to be performed more smoothly with learning and practicing. Actually, they successfully used the maximum hand motion smoothness as the performance criterion in hand reaching motion simulation (Flash and Hogan, 1985). Based on these, both minimum physical effort and maximum smoothness of the lifted load motion may play important roles in lifting motion planning. Therefore, better predictions on lifting motions might be expected when using the combination of the two performance criteria (i.e., minimum physical effort and maximum load motion smoothness) in the optimization procedure.

The two performance criteria are integrated using the weighted-sum MOO approach (Marler and Arora, 2004) for motion simulation. Specifically, two single objective functions (i.e., Obj_{Effort} and Obj_{Smooth}) are defined corresponding to the two performance criteria (i.e., minimum physical effort and maximum load smoothness), respectively. A composite objective function (Obj_{Com}) that is a function of the two single objective functions and their corresponding weightings (w_E and w_S) is minimized in the MOO procedure to generate the simulated motions. The optimization problem in this study can be presented as follows (Eq. (2)):

$$\begin{aligned} &\text{Find} && \theta_i(t) && i = 1, \ldots, 5 \\ &\text{Minimize} && Obj_{Com} = F\left(Obj_{Effort}, Obj_{Smooth}, w_E, w_S\right) \\ &\text{Subject to} && Con_j^{Eq}(\theta_i) = 0 && j = 1, \ldots, m \\ & && Con_k^{Ineq}(\theta_i) \le 0 && k = 1, \ldots, n \end{aligned} \tag{2}$$

where $\theta_i(t)$ are the joint angular trajectories; w_E and w_S are the weightings for Obj_{Effort} and Obj_{Smooth} in the MOO, respectively; $F(\cdot)$ indicates that Obj_{Com} is a function of the single objective functions (Obj_{Effort} and Obj_{Smooth}) and their weightings (w_E and w_S); Con_j^{Eq} and Con_k^{Ineq} are equality and inequality constraints, respectively. The

definitions of the single objective functions, the formulation of the composite objective function and the various constraints are presented in details as follows.

3.2.1. Objective functions

3.2.1.1. Single objective functions. Two single objective functions are defined corresponding to the two performance criteria: minimum physical effort and maximum smoothness of the load motion. The objective function of minimum physical effort (Obj_{Effort}) is defined as the time integral of the square sum of the ratios between the joint moments and the corresponding joint strengths (Eq. (3)):

$$Obj_{Effort} = \int_0^T \sum_{i=1}^{5} \left(\frac{M_i(t)}{S_i}\right)^2 dt \tag{3}$$

where M_i is the moment of joint i, S_i is the strength of joint i, and T is the total lifting time duration. The joint moment M_i can be calculated from the joint angular trajectories $\theta_i(t)$ using Eq. (1), and the joint strengths S_i were defined as the 50th percentile of the corresponding static joint moment strengths of the males or females according to Chaffin et al. (2006).

The objective function Obj_{Smooth} is defined as minimizing the jerk (i.e., maximizing the smoothness) of the end-effector (i.e. the hands and lifted load) motion. The mathematical equation of this objective function is (Eq. (4)):

$$Obj_{Smooth} = \int_0^T \left(\left(\frac{d^3x_L}{dt^3}\right)^2 + \left(\frac{d^3y_L}{dt^3}\right)^2\right) dt \tag{4}$$

in which x_L and y_L are the horizontal and vertical coordinates of the load geometric centre, respectively.

3.2.1.2. Formulation of the composite objective function. The composite objective function Obj_{Com} is defined as a weighted sum of the single objective functions Obj_{Effort} and Obj_{Smooth} after normalization (Eq. (5)):

$$\begin{aligned} &Obj_{Com} = w_E N\left(Obj_{Effort}\right) + w_S N(Obj_{Smooth}) \\ &w_E + w_S = 1 \end{aligned} \tag{5}$$

where w_E and w_S are the weightings for Obj_{Effort} and Obj_{Smooth}, respectively, with their ranges from 0 to 1. $N(\cdot)$ is a normalization operator defined by Marler and Arora (2005). Specifically, the normalization of a single objective function $N(Obj_{Sp})$ ($p = 1$ or 2) is defined as follows (Eq. (6)):

$$N\left(Obj_{Sp}\right) = \frac{Obj_{Sp}(\theta_i(t)) - Obj_{Sp}^{Min}}{Obj_{Sp}^{Max} - Obj_{Sp}^{Min}} \tag{6}$$

where Obj_{Sp}^{Min} is the minimum value of Obj_{Sp}, and Obj_{Sp}^{Max} is defined as $Obj_{Sp}(\theta_i(t)^*)$ where $\theta_i(t)^*$ is the point that minimizes the other single objective function Obj_{Sq} ($q = 1$ or 2; $q \neq p$).

3.2.2. Constraints

The constraints of the optimization consist of joint angle limits, data-based joint angular velocity constraints, joint moment limits, postural balance constraints, and body-load and shelf-load collision avoidance. Descriptions of these constraints are presented below and can also be found in our earlier work (Song et al., 2015).

3.2.2.1. Joint angle limits. The constraints of joint angle limits are defined as follows (Eq. (7)):

$$\alpha_i^L \leq \alpha_i(t) \leq \alpha_i^U \qquad i = 1, \ldots, 5, \quad t \in [0, T] \tag{7}$$

in which α_i ($i = 1, \ldots, 5$) are the included joint angles, α_i^L and α_i^U are the lower and upper boundaries of the *i-th* included joint angle, and T is the total time duration of the lifting task.

The included joint angles are the relative angles between their adjacent segments (Fig. 3(c)), and can be calculated from the joint angles θ_i using the equations in Table 2. Their boundary values (i.e., α_i^L and α_i^U presented in Table 2) were obtained from Chaffin et al. (2006).

3.2.2.2. Data-based joint angular velocity constraints. The data-based joint angular velocity constraints which were defined in Song et al. (2015) are also used in this study. Specifically, the time functions of the included joint angular velocities ($\dot{\alpha}_i(t), i = 1, \ldots, 5$) of the simulated motions are bounded by a set of functional constraints which are defined based on the actual motions in the lifting motion database.

To define these data-based constraints, a regression model is first developed based on the data in the lifting motion database using a functional regression technique (Faraway, 1997). The response variables of the regression model are the time functions of the included joint angular velocities $\dot{\alpha}_i(\tau)$, where τ is the normalized time with $\tau = 0$ and $\tau = 1$ corresponding to the start and the end of the motion, respectively. The predictors in the regression are defined by load weight, destination height, and age. A quadratic regression model is developed as follows (Eq. (8))

$$\begin{aligned} \dot{\alpha}_i^M(\tau) =& \beta_i^0(\tau) + \beta_i^W(\tau)W + \beta_i^H(\tau)H + \beta_i^A(\tau)A + \beta_i^{W^2}(\tau)W^2 \\ &+ \beta_i^{H^2}(\tau)H^2 + \varepsilon_i(\tau) \qquad i = 1, \ldots, 5; \quad \tau \in [0, 1] \end{aligned} \tag{8}$$

where $\dot{\alpha}_i^M(\tau)$ is the response variable which denotes the predicted mean value of the *i-th* included joint angular velocity at the normalized time τ; W, H and A are the predictors: W is the load weight defined as the percentage of the subject's maximum lifting capacity, H is the destination height calculated as the percentage of the body height, A is a binary accounting for the subject's age: 0 = younger adults and 1 = older adults; β_i^0, β_i^W, β_i^H, β_i^A, $\beta_i^{W^2}$, $\beta_i^{H^2}$, ε_i are the estimated time functions from the regression analysis, and $\varepsilon_i(\tau)$ is the estimated standard deviation of $\dot{\alpha}_i^M(\tau)$.

Given the total lifting duration T, the functions with normalized time τ (i.e., $\dot{\alpha}_i^M(\tau)$ and $\varepsilon_i(\tau)$) are transformed to the functions with absolute time t (i.e., $\dot{\alpha}_i^M(t)$ and $\varepsilon_i(t)$) by replacing τ with t/T. The joint angular velocity constraints are defined as follows (Eq. (9)):

$$\dot{\alpha}_i^M(t) - 1.96\varepsilon_i(t) \leq \dot{\alpha}_i(t) \leq \dot{\alpha}_i^M(t) + 1.96\varepsilon_i(t) \quad t \in [0, T] \tag{9}$$

where $\dot{\alpha}_i(t)$ is the predicted included angular velocity of the *i-th* joint at the time point t, and $[\dot{\alpha}_i^M(t) - 1.96\varepsilon_i(t),\ \dot{\alpha}_i^M(t) + 1.96\varepsilon_i(t)]$ defines the 95% confidence interval.

Table 2
Motion ranges of the included joint angles (°).

Included joint angles	Lower bound (α_i^L)	Upper bound (α_i^U)
Elbow: $\alpha_1 = 180 - \theta_1 + \theta_2$	38	180
Shoulder: $\alpha_2 = 180 - \theta_3 + \theta_2$	−61	188
Hip: $\alpha_3 = 180 - \theta_4 + \theta_3$	67	180
Knee: $\alpha_4 = 180 - \theta_4 + \theta_5$	67	180
Ankle: $\alpha_5 = \theta_5$	55	128

3.2.2.3. Joint moment limits. The joint moments are assumed to be smaller than their corresponding strengths during the whole lifting period. Therefore, the constraints on the joint moment limits are defined as follows (Eq. (10)):

$$M_i^2(t) - S_i^2 \le 0 \qquad i = 1, ..., 5, \quad t \in [0, T] \tag{10}$$

where M_i and S_i are the moment and static strength of the *i-th* joint in Eq. (3), respectively.

3.2.2.4. Postural stability constraints. The postural stability is achieved by enforcing the horizontal COM position of the body-load system to remain within the foot supporting area (Lin et al., 1999). Therefore, the postural stability constraints can be defined as follows (Eq. (11)):

$$x_{Heel} \le x_{COM}(t) \le x_{Toe} \qquad t \in [0, T] \tag{11}$$

where x_{COM} is the horizontal position of the centre of mass for the body-load system, x_{Heel} and x_{Toe} are the horizontal positions of the corresponding reflective markers (i.e., the markers at the heel and 5th metatarsal), respectively. The body COM is defined as the weighted sum of each body segment's COM. The parameters for estimating body segments' COM positions are derived from de Leva (1996). The load COM is determined as the geometric centre of the box.

3.2.2.5. Body-load collision avoidance. The collision between the human body (trunk, thigh and shank) and the lifted load should be avoided to achieve smooth lifting. Therefore, one of the constraints is defined by body-load collision avoidance. The lifted load in this study is a square box (width × height: 0.24 m × 0.26 m). For simplicity, the box dimension is approximated to be a circle (Circle A in Fig. 4) with its centre at the box geometric centre and its diameter as the length of the longer side (i.e., height). The trunk in the sagittal plane is modelled as a rectangle, and the thigh and shank are modelled as two cylinders (the dashed lines in Fig. 4), with their segment lines (i.e. the solid lines in Fig. 4) at the centre. The width of the trunk rectangle (l_1 in Fig. 4) and the diameters of the thigh and shank cylinders (l_2 and l_3 in Fig. 4) are estimated from the measured reflective marker positions in the same way as in Song et al. (2015). Specifically, the trunk width is calculated as the distance from the ASIS to the PSIS in the sagittal plane; the thigh and shank diameters are approximated as the distance between the lateral and medial epicondyles of femur. Thus, the body-load collision avoidance constraints are defined as follows (Eq. (12)):

$$\begin{aligned} \left\| \mathbf{P}_{Body}(t) - \mathbf{P}_{BC}(t) \right\| &\ge 1/2\,(H_{Box} + l_1) \\ \left\| \mathbf{P}_{Body}(t) - \mathbf{P}_{BC}(t) \right\| &\ge 1/2\,(H_{Box} + l_2) \qquad t \in [0, T] \\ \left\| \mathbf{P}_{Body}(t) - \mathbf{P}_{BC}(t) \right\| &\ge 1/2\,(H_{Box} + l_3) \end{aligned} \tag{12}$$

where $\mathbf{P}_{Body}$ is the position of any point on the trunk, thigh or shank segment lines; $\mathbf{P}_{BC}$ is the position of the box centre, $\|\|$ denotes the Euclidean distance between $\mathbf{P}_{Body}$ and $\mathbf{P}_{BC}$; H_{Box} is the box height; and l_1, l_2 and l_3 represent the trunk width, the diameters of the thigh and shank, respectively (Fig. 4).

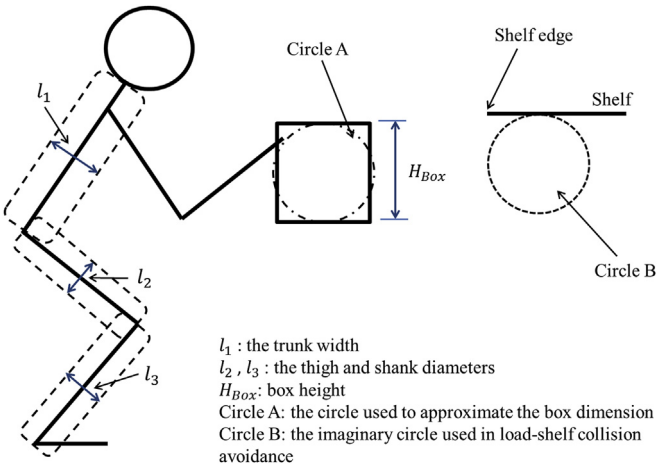

Fig. 4. The definitions of the body-load and shelf-load collision avoidance constraints.

3.2.2.6. Shelf-load collision avoidance. To define the constraint of the shelf-load collision avoidance, an imaginary circle is placed right below the shelf (Circle B in Fig. 4), and the box should bypass this circle during lifting. The circle was tangent to the shelf, and its diameter is set as the same as the box height. The horizontal distance from the circle centre to the shelf edge is the circle radius. The lifted box is approximated in the same way as in the body-load collision avoidance constraints. Thus, the constraints of the shelf-load collision avoidance can be defined by calculating the distance from the box centre to the imaginary circle centre (Eq. (13)):

$$\|\mathbf{P}_{BC}(t) - \mathbf{P}_{CC}\| \ge 1/2\,(H_{Box} + D_{Circle}) \qquad t \in [0, T] \tag{13}$$

where $\mathbf{P}_{BC}$ is the position of the box centre, $\mathbf{P}_{CC}$ is the position of the imaginary circle centre, H_{Box} is the box height, and D_{Circle} is the diameter of the imaginary circle.

3.3. Joint angular trajectory model

Human motions are composed of infinite postures changing with time. Therefore, the optimization problem in Eq. (2) is actually of infinite dimension. To deal with this infinite-dimension problem, the joint angular trajectories are represented using polynomial functions, and the parameters in these functions become the design variables in the optimization procedure. Specifically, each joint angular trajectory $\theta_i(t)$ is represented by a seventh-order Hermite polynomial (Kincaid and Cheney, 2002) interpolated by the joint angles at certain time points during lifting (Eq. (14)):

$$\begin{aligned} &\theta_i(t) = f(\theta_{i0}, \theta_{iT}, \theta_i(t_l), T, t) \qquad i = 1, ..., 5 \\ &\dot{\theta}_{i0} = \dot{\theta}_{iT} = 0 \end{aligned} \tag{14}$$

in which θ_{i0} and θ_{iT} are the joint angles in the starting and ending postures, respectively; t_l represents the time points at 20%, 40%, 60% and 80% of the total time duration T; $\dot{\theta}_{i0}$ and $\dot{\theta}_{iT}$ are the initial and final joint angular velocities which are assumed to be zero.

Therefore, the optimization problem in Eq. (2) is transformed into a simplified one where the design variables are defined by twenty joint angles $\theta_i(t_l)$ and denoted as a vector $\boldsymbol{\theta}$ (Eq. (15)):

$$\begin{aligned} &\text{Find} \quad \boldsymbol{\theta} \\ &\text{Minimize} \quad Obj_{Com} = F\left(\boldsymbol{\theta}, Obj_{Effort}, Obj_{Smooth}, w_E, w_S\right) \\ &\text{Subject to} \quad Con_j^{Eq}(\boldsymbol{\theta}) = 0 \qquad j = 1, ..., m \\ &\qquad\qquad Con_k^{Ineq}(\boldsymbol{\theta}) \le 0 \qquad k = 1, ..., n \\ &\boldsymbol{\theta} = [\theta_1(t_1), \theta_1(t_2), ..., \theta_i(t_l), ..., \theta_5(t_4)] \qquad i = 1, ..., 5 \\ &t_l = 0.2T, 0.4T, 0.6T, 0.8T, \qquad\qquad l = 1, ..., 4 \end{aligned} \tag{15}$$

3.4. Simulation process

The whole simulation process for one lift with pre-specified weighting values (w_E and w_S) is illustrated in Fig. 2. At the beginning, the functional regression equations (Eq. (8)) are first determined using the actual motions in the database. Given the task condition (i.e., load weight and destination height), the participant's attributes (i.e., age, body height and MLC), and the total lifting time duration, the functional parameters $\alpha_i^M(t)$ and $\varepsilon_i(t)$ are calculated using Eq. (8), and will be further used to construct the data-based joint angular velocity constraints for the optimization model.

The initial values of the design variable vector ($\boldsymbol{\theta_0}$) are determined using actual motions selected from the motion database. It should be noted that the selected actual motions must be consistent with the simulated one in age attribute (younger or older) and task scenario (i.e., load weight and destination height). Multiple motion trials could be retrieved from the database for simulating one lift. If this is the case, these trials are used to simulate the lifting motions of interest separately. The simulated motion that generates the minimum value of the composite objective function (Eq. (5)) is selected as the final prediction result.

Once the initial values of the design variable vector ($\boldsymbol{\theta_0}$) and the data-based constraints ($\alpha_i^M(t)$,$\varepsilon_i(t)$) are determined, the lifting motions are simulated by solving the optimization problem (Eq. (15)) using an iterative searching method. This iteration process is illustrated as in the dashed-line square in Fig. 2. The iteration starts with the inputs including the initial values of the design variable vector $\boldsymbol{\theta_0}$, the starting and ending body postures, the total time duration and the weightings w_E and w_S. In each searching iteration, the joint angular trajectories $\theta_i(t)$ are first formulated based on the inputs using the joint angular trajectory model. The joint angular trajectories $\theta_i(t)$ are then sent to the physical human body model to calculate various kinematic and kinetic variables, including the joint moments, the included joint angles and velocities, the box motion trajectory and the whole body configurations throughout the total lifting duration. These variables are used to evaluate the objective functions and constraints in the optimization model. The optimization model generates intermediate design variable vector $\boldsymbol{\theta}_{Inter}$ after each searching iteration. Finally, the optimal design variable vector $\boldsymbol{\theta}_{Optim}$ are predicted by minimizing the composite objective function subject to all the constraints. The optimization is solved using the sequential quadratic programming algorithm (SQP) implemented by the optimization toolbox in MATLAB, and the gradients of the objective function and constraints were calculated numerically.

4. Motion simulation and model evaluation

The 238 motions of 10 participants mentioned in Section 2 were simulated and used to evaluate the model performance. To examine the effects of the weightings on the prediction results, a series of weighting values in the composite objective function (Eq. (5)) were evaluated in the simulation. Specifically, the weightings were ranged from 0 to 1 with an equal interval of 0.1:

$$w_E = 0 : 0.1 : 1, \quad w_S = 1 - w_E \tag{16}$$

The model performance was evaluated by comparing the simulated motions with their corresponding actual ones. The discrepancy between these two was quantified using the root-mean-squared (RMS) absolute joint angle errors. The errors of the predicted motions based on different weightings were compared within younger and older groups, respectively, so as to determine the optimal weightings for each age group.

5. Simulation results

Fig. 5 shows the mean RMS absolute angular errors of all joints combined (i.e., overall error) between the simulated and actual motions for different weighting values in the younger and older age groups. When using Obj_{Effort} (i.e., $w_E = 1.0$ and $w_S = 0$) and Obj_{Smooth} (i.e., $w_E = 0$ and $w_S = 1.0$) as the single objective functions, the overall RMS absolute joint angle errors in the older adults are 12.33° and 11.26°, respectively. After using the MOO approach, the error for the older subjects decreases to the lowest level at 10.01° when $w_E = 0.1$ and $w_S = 0.9$. For the younger subjects, the minimum overall RMS error across different weightings is 9.37° when $w_E = 0.9$ and $w_S = 0.1$ (Fig. 5). The overall errors are 9.55° and 11.55° when only using Obj_{Effort} and Obj_{Smooth} in the single objective optimization, respectively.

Table 3 illustrates the mean, median, minimum and maximum overall RMS joint angle errors under varied task conditions when using the overall optimal weightings for younger ($w_E = 0.9$ and $w_S = 0.1$) and older ($w_E = 0.1$ and $w_S = 0.9$) subjects, respectively. Table 4 presents the mean RMS angular errors for each joint under varied task scenarios under the overall optimal weightings for both age groups. Comparisons between the actual and simulated motions for two representative lifting trials were illustrated in Fig. 6. These trials were performed by one younger and one older adult, respectively, with the load weight of 15% MLC and the shelf height at the elbow level. The optimal weightings in the MOO approach (i.e. younger adult: $w_E = 0.9$ and $w_S = 0.1$; older adult: $w_E = 0.1$ and $w_S = 0.9$) were used in the simulation for these two trials.

6. Discussion

The major purpose of this study was to develop a novel lifting motion simulation model based on the MOO approach. A new combination of performance criteria, minimum physical effort and maximum load motion smoothness, was examined using the weighted-sum MOO approach. Lifting motions performed by younger and older adults under varied task conditions were simulated. The comparisons between the simulated and corresponding actual motions were made using their absolute RMS joint angle errors for evaluating the performance of this model. The optimal weightings in the MOO associated with the minimum simulation errors were determined for younger and older adults separately.

The MOO approach which integrates the two performance measures (i.e., physical effort and load motion smoothness) successfully reduces the prediction errors for both younger and older age groups compared with using the single-objective optimization. In the younger group, compared to using Obj_{Effort} and Obj_{Smooth} alone in the single-objective optimization, the overall RMS absolute joint angle error decreases by up to 1.9% and 18.9% (when $w_E = 0.9$ and $w_S = 0.1$), respectively, when using the MOO approach. For older adults, the MOO approach reduced the overall error by up to 18.8% and 11.1% (when $w_E = 0.1$ and $w_S = 0.9$) compared to the single objective optimization approaches using Obj_{Effort} and Obj_{Smooth} alone, respectively. Such reduction in the overall RMS absolute joint angle error supported the argument made by Chang et al. (2001) that more than one performance criterion might be needed to better predict and explain the lifting behaviour. In addition, it also suggested that a combination of minimum physical effort and maximum load motion smoothness could be an effective way to define the objective function in the MOO approach for better lifting motion prediction.

The age-related differences in the optimal combinations of the performance measures in the MOO approach may help better understand the distinctions between younger and older adults

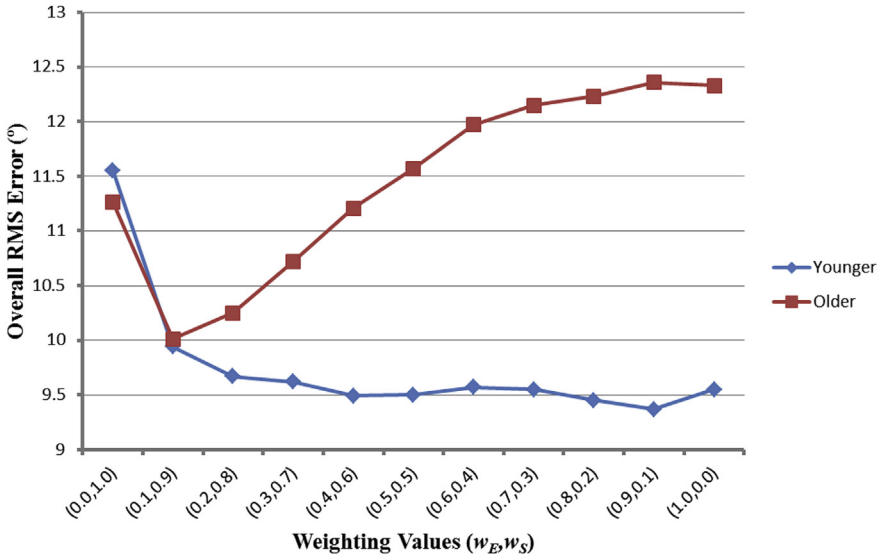

Fig. 5. The mean RMS absolute joint angle errors (°) under different weighting values for the younger and older age groups.

Table 3
Mean, median, minimum and maximum absolute joint angle RMS errors (°).

	The number of trials	Mean	Median	Minimum	Maximum
Age					
Younger	123	9.37	8.84	4.98	23.42
Older	115	10.01	10.17	5.09	15.99
Load weight					
5% MLC	75	9.43	9.25	4.98	17.33
15% MLC	84	9.71	9.68	5.09	23.42
25% MLC	79	9.87	9.38	5.18	15.99
Shelf height					
Wrist	83	10.22	10.62	5.37	16.38
Elbow	84	9.35	9.20	4.98	15.49
Shoulder	71	9.42	8.84	5.09	23.42
Overall	238	9.68	9.53	4.98	23.42

The weightings for younger adults: $w_E = 0.9$ and $w_S = 0.1$; the weightings for older adults: $w_E = 0.1$ and $w_S = 0.9$.

regarding their motor control mechanisms during lifting. The physical effort is closely associated with the energy expenditure during lifting tasks (Fogleman and Smith, 1995); while minimizing load motion jerk during lifting is related with decreased spinal compressive forces (Hsiang and McGorry, 1997). For the younger adults, the optimal weightings of the physical effort and load motion jerk are 0.9 and 0.1, respectively, which indicates that minimizing energy expenditure are the dominant objective when planning lifting motions. Given the optimal weighting values of older adults (0.1 and 0.9 for physical effort and load motion jerk, respectively), reducing low back load seems to play a more important role in older adults' lifting motion planning compared with decreasing energy expenditure.

Such age-related difference is consistent with our earlier findings (Song and Qu, 2014a) that older adults tend to use safer lifting strategies (e.g., reduced trunk flexion and lifting velocities) to reduce their low back load than do younger ones. In fact, because of age-related degenerations in trunk muscle and intervertebral discs (Adams et al., 2002; Doherty, 2003; Roughley, 2004), older adults are associated with high LBP risks (Heiden et al., 2013). Therefore, older adults tend to give the first priority to reducing the low back load when planning their lifting motions. For younger adults, their lifting motion patterns (e.g., higher trunk flexion and lifting velocities) can help decrease energy expenditure (Maduri et al., 2008; Song and Qu, 2014b) and increase working efficiency (reducing the total lifting duration), but induce larger low back loads. However, given their higher trunk muscle strengths (Singh et al., 2013), the increased loads might still be in the safe margin for younger adults. Therefore, younger adults choose more energy-saving and efficient kinematic patterns when planning lifting motions at the expense of increasing low back loads.

Compared with the optimization-based models, the hybrid model in this study increases the realism of the predicted motions by incorporating the actual human motions into the optimization framework. In particular, the joint angular trajectories are constrained by the time-functional boundaries determined by real lifting motions. Chaffin (2005) argued that human motion simulation models should be based on real motion data to assure their validity. Pasciuto et al. (2014) and Xiang et al. (2012b) also showed that the hybrid approach can generate more realistic predictions and improve the simulation accuracy compared to the purely optimization-based approach. On the other hand, the hybrid approach has its own drawback: a database of actual human motions is required. However, as shown in the current and previous studies (Pasciuto et al., 2014; Song et al., 2015; Xiang et al., 2012b), the hybrid approach is able to simulate motions in novel scenarios which are different from those in the database. Pasciuto et al. (2014)

Table 4
Mean absolute joint angle RMS errors (°).

	Elbow	Shoulder	Hip	Knee	Ankle
Age					
Younger	12.74	11.41	6.52	5.14	4.37
Older	14.17	13.66	5.68	4.41	4.25
Load weight					
5% MLC	13.24	12.05	5.39	4.98	4.71
15% MLC	13.26	13.08	6.02	4.81	4.17
25% MLC	13.80	12.30	6.90	4.57	4.08
Shelf height					
Wrist	16.30	11.43	6.54	4.22	3.66
Elbow	11.19	13.87	6.16	5.01	3.96
Shoulder	12.74	12.12	5.60	5.17	5.49
Overall	13.43	12.50	6.11	4.79	4.31

The weightings for younger adults: $w_E = 0.9$ and $w_S = 0.1$; the weightings for older adults: $w_E = 0.1$ and $w_S = 0.9$.

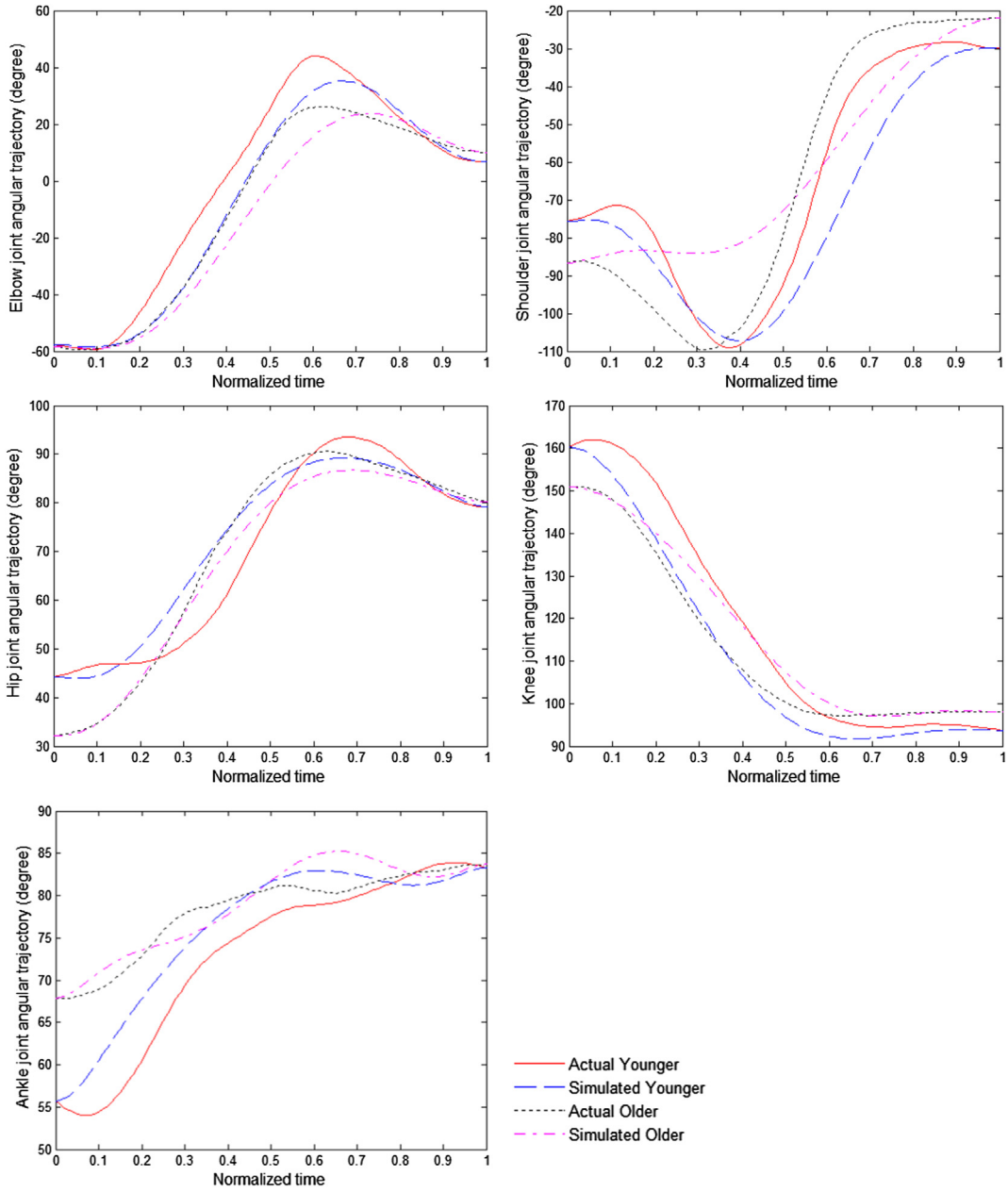

Fig. 6. The actual and simulated joint angular trajectories for one younger and older adult, with load weight of 15% MLC and shelf height at the elbow level; the weightings used in the MOO are $w_E = 0.9$ and $w_S = 0.1$ for the younger adult and $w_E = 0.1$ and $w_S = 0.9$ for the older adult.

indicated that the use of the knowledge-based objective function in the hybrid approach could reduce the prediction dependency on the goodness of the actual human motions in the database (i.e., improving the extrapolation capability).

Xiang et al. (2010) also proposed a lifting motion simulation model by using the MOO approach. However, they only used the model to simulate lifting motions of young and middle-aged adults. In addition, the performance criteria used in their model appeared not good enough as they found that the addition of the maximum stability in the objective function did not significantly improve simulation accuracy. The present study is superior to Xiang et al. (2010) mainly in two aspects. First, we simulated lifting motions for both younger and older adults, and attempted to use the proposed model to identify age-related differences in lifting motion planning. As the workforce is ageing worldwide and older workers tend to have higher risks of LBP, the knowledge on age-related differences in lifting motion planning is important for occupational LBP prevention. Second, previous research suggests that reducing low back load plays an important role in older adults' lifting motion planning (Song and Qu, 2014a), and minimizing load motion jerk is closely associated with reducing low back load (Hsiang and McGorry, 1997). Thus, minimum load motion jerk was included in the objective function of the optimization procedure. These findings provide an experimental basis for the inclusion of minimum load motion jerk in the objective function of the optimization procedure which enhances the validity of our proposed model.

There are several limitations in this study. First, comprehensive data of age-specific dynamic strengths for the lifting task is not available in the existing literature. Therefore, only static strength

was used and age-related differences in the joint strengths were not taken into account when defining the objective functions. This could have adverse effects on the simulation results. To obtain better simulation accuracy, dynamic joint strength data of different age populations should be measured and used in future motion simulation models. Second, only static postural stability constraint (Lin et al., 1999) was applied in this study. The dynamic stability based on zero moment point (Xiang et al., 2010) should be used in future studies. Third, only 2-D sagittal lifting motions were simulated. Lifting outside the sagittal plane (i.e. asymmetric lifting) is common in industry, and associated with higher LBP risks (Davis and Marras, 2005). Therefore, the present model should be further developed for simulating 3-D lifting motions in future research. Specifically, a complex 3-D human body model with more degrees of freedom will be adopted for simulating 3-D asymmetric lifting motions in our future study. In addition, only two performance criteria were examined using the MOO approach in this study. Other performance criteria, such as minimum joint torque change (Uno et al., 1989), minimum muscle force change (Menegaldo et al., 2003) and minimum spine compressive force (Xiang et al., 2012a) may also be investigated in the MOO approach in future studies so as to better understand the mechanisms of lifting motion planning. In order to do so, various musculoskeletal human body models, such as biomechanical muscle models (Delp et al., 1990) and musculoskeletal spine models (Chaffin et al., 2006), should be integrated into the present motion prediction model. Finally, as suggested by Chaffin (2005), fast computation for real time simulations is one of the most important criteria when evaluating digital human models for proactive ergonomics. Therefore, other optimization algorithms could be used in future research, and post-optimization analysis on various computation parameters (e.g., CPU time, number of iterations) will be conducted in future simulations to evaluate the computation efficiency of different optimization algorithms.

7. Conclusions

In this study, a novel lifting motion simulation model was developed using the MOO approach. A combination of two performance criteria, minimum physical effort and maximum load motion smoothness, was examined using the weighted-sum MOO approach. Two-dimensional lifting motions performed by younger and older adults under varied task conditions were simulated. The optimal weightings in the MOO that led to the best simulation accuracy were determined separately for both age groups. The results showed that using the MOO approach improved the simulation accuracy compared with using the single-objective optimization approach. The MOO approach also helps provide insight into how humans of different ages plan and control lifting motions. In particular, minimizing physical effort plays a more important role than maximizing load motion smoothness during lifting motion control for younger adults. For older adults, however, maximum load motion smoothness seems to be a dominant objective during lifting tasks.

Acknowledgements

This study was conducted at Nanyang Technological University and was supported in part by the Academic Research Fund from Ministry of Education, Singapore (Project Reference: 2013-T1-002-068).

References

Abdel-Malek, K., Yang, J., Marler, T., Beck, S., Mathai, A., Zhou, X., Patrick, A., Arora, J., 2006. Towards a new generation of virtual humans. Int. J. Hum. Factors Model. Simul. 1 (1), 2–39.
Abedi, P., Shoushtari, A.L., Bistooni, M., 2012. Posture prediction of humanoid robot: modeling and simulation of manual lifting. In: Information and Automation (ICIA), 2012 International Conference on IEEE, pp. 536–541.
Adams, M.A., Bogduk, N., Burton, K., Dolan, P., 2002. Biology of spinal tissues (Chapter 4). In: The Biomechanics of Back Pain. Churchill Livingstone, Edinburgh.
Chaffin, D.B., 2005. Improving digital human modelling for proactive ergonomics in design. Ergonomics 48 (5), 478–491.
Chaffin, D.B., Andersson, G.B.J., Martin, B.J., 2006. Occupational Biomechanics, fourth ed. Wiley, New York.
Chang, C.C., Brown, D.B., Bloswick, D.S., Hsiang, S.M., 2001. Biomechanical simulation of manual lifting using spacetime optimization. J. Biomech. 34, 527–532.
Davis, K.G., Marras, W.S., 2005. Load spatial pathway and spine loading: how does lift origin and destination influence low back response? Ergonomics 48, 1031–1046.
de Leva, P., 1996. Adjustments to Zatsiorsky-Seluyanov's segment inertia parameters. J. Biomech. 29, 1223–1230.
Delp, S.L., Loan, J.P., Hoy, M.G., Zajac, F.E., Topp, E.L., Rosen, J.M., 1990. An interactive graphics-based model of the lower extremity to study orthopaedic surgical procedures. IEEE Trans. Biomed. Eng. 37 (8), 757–767.
Doherty, T.J., 2003. Invited review: aging and sarcopenia. J. Appl. Physiol. 95 (4), 1717–1727.
Dysart, M.J., Woldstad, J.C., 1996. Posture prediction for static sagittal-plane lifting. J. Biomech. 29, 1393–1397.
Faraway, J.J., 1997. Regression analysis for a functional response. Technometrics 39, 254–261.
Flash, T., Hogan, N., 1985. The coordination of arm movements: an experimentally confirmed mathematical model. J. Neurosci. 5 (7), 1688–1703.
Fogleman, M., Smith, J.L., 1995. The use of biomechanical measures in the investigation of changes in lifting strategies over extended periods. Int. J. Ind. Ergon. 16, 57–71.
Garg, A., Moore, J.S., 1992. Epidemiology of low-back pain in industry. Occ. Med. 7, 593–608.
Gündogdu, Ö., Anderson, K.S., Parnianpour, M., 2005. Simulation of manual materials handling: biomechanical assessment under different lifting conditions. Technol. Health Care 13 (1), 57–66.
Heiden, B., Weigl, M., Angerer, P., Müller, A., 2013. Association of age and physical job demands with musculoskeletal disorders in nurses. Appl. Ergon. 44 (4), 652–658.
Hoy, D., Brooks, P., Blyth, F., Buchbinder, R., 2010. The epidemiology of low back pain. Best Pract. Res. Clin. Rheumatol. 24, 769–781.
Hsiang, S.H., Ayoub, M.M., 1994. Development of methodology in biomechanical simulation of manual lifting. Int. J. Ind. Ergon. 13, 271–288.
Hsiang, S.M., McGorry, R.W., 1997. Three different lifting strategies for controlling the motion patterns of the external load. Ergonomics 40, 928–939.
Jung, E.S., Shin, Y., 2010. Two handed human reach prediction models for ergonomic evaluation. Hum. Factors Ergon. Manuf. Serv. Ind. 20 (3), 192–201.
Jung, E.S., Kee, D., Chung, M.K., 1995. Upper body reach posture prediction for ergonomic evaluation models. Int. J. Ind. Ergon. 16 (2), 95–107.
Katz, J.N., 2006. Lumbar disc disorders and low-back pain: socioeconomic factors and consequences. J. Bone Jt. Surg. 88 (Suppl. 2), 21–24.
Kincaid, R.D., Cheney, E.W., 2002. Numerical Analysis: Mathematics and Scientific Computing, third ed. American Mathematical Society, Providence, Rhode Island.
Krismer, K., van Tulder, M., 2007. Low back pain (non-specific). Best Pract. Res. Clin. Rheumatol. 21, 77–91.
Lin, C.J., Ayoub, M.M., Bernard, T.M., 1999. Computer motion simulation for sagittal plane lifting activities. Int. J. Ind. Ergon. 24, 141–155.
Maduri, A., Pearson, B.L., Wilson, S.E., 2008. Lumbar–pelvic range and coordination during lifting tasks. J. Electromyogr. Kinesiol. 18 (5), 807–814.
Marler, R.T., Arora, J.S., 2004. Survey of multi-objective optimization methods for engineering. Struct. Multidiscip. Optim. 26, 369–395.
Marler, R.T., Arora, J.S., 2005. Function-transformation methods for multi-objective optimization. Eng. Optim. 37, 551–571.
Menegaldo, L.L., Fleury, A.D.T., Weber, H.I., 2003. Biomechanical modeling and optimal control of human posture. J. Biomech. 36, 1701–1712.
Mi, Z., Yang, J.J., Abdel-Malek, K., 2009. Optimization-based posture prediction for human upper body. Robotica 27 (04), 607–620.
Pasciuto, I., Ausejo, S., Celigüeta, J.T., Suescun, Á., Cazón, A., 2014. A comparison between optimization-based human motion prediction methods: data-based, knowledge-based and hybrid approaches. Struct. Multidiscip. Optim. 49 (1), 169–183.
Qu, X., Nussbaum, M.A., 2009. Simulating human lifting motions using fuzzy-logic control. IEEE Trans. Syst. Man Cybern. A Syst. Hum. 39, 109–118.
Roughley, P.J., 2004. Biology of intervertebral disc aging and degeneration: involvement of the extracellular matrix. Spine 29 (23), 2691–2699.
Singh, D.K., Bailey, M., Lee, R., 2013. Decline in lumbar extensor muscle strength in older adults: correlation with age, gender and spine morphology. BMC Musculoskelet. Disord. 14 (1), 215.
Song, J., Qu, X., 2014a. Effects of age and its interaction with task parameters on lifting biomechanics. Ergonomics 57, 653–668.
Song, J., Qu, X., 2014b. Age-related biomechanical differences during asymmetric lifting. Int. J. Ind. Ergon. 44, 629–635.
Song, J., Qu, X., Chen, C.H., 2015. Lifting motion simulation using a hybrid approach.

Ergonomics 58 (9), 1557–1570.
Uno, Y., Kawato, M., Suzuki, R., 1989. Formation and control of optimal trajectory in human multijoint arm movement. Biol. Cybern. 61, 89–101.
Xiang, Y., Arora, J.S., Rahmatalla, S., Abdel-Malek, K., 2009. Optimization-based dynamic human walking prediction: one step formulation. Int. J. Numer. Methods Eng. 79 (6), 667–695.
Xiang, Y., Arora, J.S., Abdel-Malek, K., 2012a. 3D human lifting motion prediction with different performance measures. Int. J. Hum. Robot. 09, 1250012.
Xiang, Y., Arora, J.S., Abdel-Malek, K., 2012b. Hybrid predictive dynamics: a new approach to simulate human motion. Multibody Syst. Dyn. 28 (3), 199–224.
Xiang, Y., Arora, J.S., Salam, R., Marler, T., Bhatt, R., Abdel-Malek, K., 2010. Human lifting simulation using a multi-objective optimization approach. Multibody Syst. Dyn. 23, 431–451.